

A STUDY OF DEADBEAT TERMINAL CONTROL FOR HIGH SPEED LOW VIBRATION ROBOTS¹

Richard W. Longman², George Klein, John Luk
Designatronics, Inc., New Hyde Park, N.Y. 11040

Sun Jian-Guo³, Zhang Lie-Ping⁴

Columbia University, New York, N.Y. 10027

Abstract

The primary limitation to increasing the operating speeds of robots, and hence their productivity, is the vibrations induced by high accelerations. Since these vibrations are usually only important near the endpoint of the arm trajectory, this paper proposes the use of a separate controller for this part of the trajectory, specifically designed for vibration control. This makes use of the fact that in the neighborhood of the endpoint the system can be considered linear. To solve the modeling problems accurate for the current endpoint and load conditions, it is proposed that a robot operator conduct a test run during which data is automatically taken. It is later used off-line by the robot microprocessor to obtain the system model in the neighborhood of the endpoint, and the feedback control gains. A deadbeat control law is studied here because of its time optimality and because it has a feedback form. The research here establishes, both by simulation and by experimental testing, that the overall approach has considerable promise. However, some new development is needed in the control law design to realize its promise.

DISTRIBUTION STATEMENT A

Approved for public release
Distribution Unlimited

DTIC
S ELECTE D
DEC 29 1988
C₀D

1. Research supported in part by DARPA SBIR Contract No. N00014-85-C-0897 to Designatronics, Inc.
2. Consultant. Also, Professor of Mechanical Engineering, Columbia University, N.Y., N.Y. 10027.
3. Visiting Scholar, Department of Mechanical Engineering, on leave from Nanjing Aeronautical Institute, Nanjing, PRC.
4. Visiting Scholar, Department of Mechanical Engineering, on leave from Xian Jiaotong University, PRC.

REPORT DOCUMENTATION PAGE

Form Approved
OMB No. 0704-0188
Exp. Date: Jun 30, 1986

1a. REPORT SECURITY CLASSIFICATION Unclassified			1b. RESTRICTIVE MARKINGS		
2a. SECURITY CLASSIFICATION AUTHORITY			3. DISTRIBUTION/AVAILABILITY OF REPORT Unlimited		
2b. DECLASSIFICATION/DOWNGRADING SCHEDULE					
4. PERFORMING ORGANIZATION REPORT NUMBER(S) None			5. MONITORING ORGANIZATION REPORT NUMBER(S)		
6a. NAME OF PERFORMING ORGANIZATION Designatronics Inc.		6b. OFFICE SYMBOL (If applicable)	7a. NAME OF MONITORING ORGANIZATION DCASMA		
6c. ADDRESS (City, State, and ZIP Code) 2101 Jericho Tpke., New Hyde Park, NY 11040			7b. ADDRESS (City, State, and ZIP Code)		
8a. NAME OF FUNDING/SPONSORING ORGANIZATION DARPA		8b. OFFICE SYMBOL (If applicable) DARPA/ISTO	9. PROCUREMENT INSTRUMENT IDENTIFICATION NUMBER N00014-85-C-0897		
8c. ADDRESS (City, State, and ZIP Code) 1400 Wilson Blvd. Arlington, VA 22209			10. SOURCE OF FUNDING NUMBERS		
PROGRAM ELEMENT NO.		PROJECT NO.	TASK NO.	WORK UNIT ACCESSION NO.	
11. TITLE (Include Security Classification) A Study of Deadbeat Terminal Control for High Speed Low Vibration Robots					
12. PERSONAL AUTHOR(S) See Over					
13a. TYPE OF REPORT Final		13b. TIME COVERED FROM Nov. 85 TO Dec. 88		14. DATE OF REPORT (Year, Month, Day) 88/12/22	
15. PAGE COUNT 37					
16. SUPPLEMENTARY NOTATION					
17. COSATI CODES			18. SUBJECT TERMS (Continue on reverse if necessary and identify by block number)		
FIELD	GROUP	SUB-GROUP	Deadbeat Control, High Speed Robot Control, Robotics		
19. ABSTRACT (Continue on reverse if necessary and identify by block number) The primary limitation to increasing the operating speeds of robots, and hence their productivity, is the vibrations induced by high accelerations. Since these vibrations are usually only important near the endpoint of the arm trajectory, this paper proposes the use of a separate controller for this part of the trajectory, specifically designed for vibration control. This makes use of the fact that in the neighborhood of the endpoint the system can be considered linear. To solve the modeling problems accurate for the current endpoint and load conditions, it is proposed that a robot operator conduct a test run during which data is automatically taken. It is later used off-line by the robot microprocessor to obtain the system model in the neighborhood of the endpoint, and the feedback control gains. A deadbeat control law is studied here because of its time optimality and because it has a feedback form. The research here establishes, both by simulation and by experimental testing, that the overall approach has considerable promise. However, some new development is needed in the control law design to realize its promise.					
20. DISTRIBUTION/AVAILABILITY OF ABSTRACT <input checked="" type="checkbox"/> UNCLASSIFIED/UNLIMITED <input type="checkbox"/> SAME AS RPT. <input type="checkbox"/> DTIC USERS			21. ABSTRACT SECURITY CLASSIFICATION Unclassified		
22a. NAME OF RESPONSIBLE INDIVIDUAL Robert Rosenfeld			22b. TELEPHONE (Include Area Code) 202-694-4001		22c. OFFICE SYMBOL DARPA/ISTO

12. Klein, George
Longman, Richard, Prof. of Mech. Eng., Columbia University
Luk, John
Sun, Jian-Guo, Visiting Scholar from Nanjing
Aeronautical Inst., Nangjing, PRC
Zhang, Lie-Ping, Visiting Scholar from
Xian Jiaotong University, PRC

INTRODUCTION

The research presented here is aimed at the problem of increasing the speed of robot operation in order to increase productivity. The productivity of manufacturing operations, and the rate of increase in productivity, are some of the major indicators of health in any nation's economy, and the productivity of any automated plant is directly affected by the speed of the robots employed.

The basic limitation in robot operating speeds using current control methods stems from the excitation of vibrations by the high accelerations and decelerations involved. The frequency of these vibrations is typically in the range of 10 to 15 Hz. Because the robot is such a highly nonlinear system, the actual frequency varies with the current robot position and load.

Present industry practice handles the vibration problem by keeping the bandwidth of the controllers for each axis sufficiently low that the vibrations are not unduly excited. Another way of saying this is that the robot motions are slowed down to move so "gently" that vibrations are not unduly excited. This produces a comparatively sluggish response -- sluggish by comparison to what would be possible with a controller specifically designed to take into account the vibrations and actively control them.

The aim of the research reported here is to develop and evaluate a methodology and one candidate for such a controller design. A method that is successful at actively handling vibrations would not only speed up current robot designs, but would also allow a second generation of increased robot speeds by allowing use of lighter and more agile arms.

The Control Philosophy

In most robot tasks the vibrations that are excited as a result of commanding high accelerations and decelerations are not of particular concern over most of the arm trajectory, and only become important when the arm is supposed to have reached its final commanded position. At this time the robot should not have to wait for the vibrations to die away before performing the needed task. This suggests that instead of trying to find a method of controlling vibrations throughout the arm's motion, a special vibration control law should be initiated as the robot arm approaches the desired end position. This approach has the following important properties:

1. In the vicinity of the final position, the highly nonlinear dynamic equations of a multibody robot model will be linear (assuming backlash and sliding friction effects to be small). This is important because there are very few



For	
RA&I	<input checked="" type="checkbox"/>
AB	<input type="checkbox"/>
iced	<input type="checkbox"/>
on	
n/	
ability Codes	
all and/or Special	

A-1

general methods in the control literature for handling highly nonlinear problems, but there is a vast body of literature that is pertinent to linear problems.

2. The approach allows faster operation of robots in the following sense: if one knows how to kill the vibrations near the end of the trajectory, one need not worry about exciting the vibrations earlier by use of high accelerations and decelerations.

We direct our attention to vibration control in three important classes of robots -- those in which the vibrations are primarily caused by the use of belt drives, or due to the use of harmonic drives, or due to structural flexibility. Many robots use belts and pulleys in the actuation mechanism to allow the placement of the motors toward the base of the arm decreasing the arm's inertia. These mechanisms are prime sources of vibration. Other robots make use of harmonic drives, because of the convenient size, the large gear ratios available, and the lack of backlash. Again, the price that is paid for these good properties is the introduction of a flexible element that produces vibrations. There are relatively few robots in the third class -- those in which the primary source of vibrations is the structural flexibility of the arm, but this class is gaining in importance as people contemplate use of ultra-lightweight composite materials with the aim of decreasing mass and inertia and increasing operating speeds. Before this goal can be accomplished, a solution to the vibration control problem must be found.

In order to generate any sophisticated control method for a specific problem, one needs to obtain the differential equations of motion describing the system to be controlled. In the case of vibration control in robots this could be a serious difficulty, because the overall equations are very complex and nonlinear, and give different vibration characteristics for each arm end-effector position considered. Furthermore, the needed equations can change substantially with the mass of the load being carried by the robot, as well as with all the parameters in the inertia tensor for the load. Hence, accurately predicting and then somehow cataloging the vibration equations for the robot in all possible operating conditions would be a large and difficult task.

Our solution to this difficulty is to have the robot operator perform a test run during which data is stored as the arm approaches its end position. This data is then analyzed to obtain a model that represents the dynamics of the system in the vicinity of the trajectory endpoint, under the prevailing

operating conditions and with the appropriate load characteristics. This analysis can be performed on a microprocessor of an IBM-PC class, which is already part of most robot manipulators, so that usually no extra computational equipment is needed. The aim is to have this identification step be something that any robot operator can perform, without needing any special expertise. To summarize, the use of this identification step:

1. Avoids the need and difficulty of careful dynamic modelling.
2. Avoids the need to predict vibration dynamics in all possible situations, and somehow store the information.
3. Avoids the stability issues and complexity associated with use of adaptive control, which is perhaps the only real competitor to the proposed method.
4. And can be performed on a microprocessor which might already be part of the robot hardware.
5. The method will require that extra sensors be placed on the robot, but these sensors would also be needed by most control laws one might consider using, and would usually be low cost.

Having got the system model needed, it remains to determine an appropriate control law to eliminate vibrations quickly. Ideally, one would like to kill the vibrations and reach the endpoint as fast as possible after the vibration control phase is initiated near the end of the arm trajectory. In other words, one would like to apply time optimal control theory. Unfortunately, it is quite difficult to find the time optimal control for any substantial system, and most methods give the control only in open loop form. One then has to use ingenuity to try to generate some kind of approximate closed loop form that can be implemented in practice. These difficulties generally preclude the use of time optimal control. On the other hand, deadbeat control is a time optimal control in a discrete time setting. It is easy to compute, and it can be computed in a feedback form. In addition, since deadbeat control is a digital control method, it is automatically in the appropriate form for implementation on the robot's microprocessor, which needs only to make a few multiplications and additions to implement in real time. This paper cites the needed theory and evaluates the effectiveness of this candidate for terminal vibration control by simulation and experiment.

To summarize, the overall aim of the control approach is to develop a control package that can be used routinely by a factory robot operator who knows nothing of control theory. During the set up procedure he inputs the desired trajectory command to the standard robot controller, and makes the

identification test run during which the robot microprocessor stores data from sensors on the robot. The microprocessor uses the data to develop a system model and from this develop feedback gains for the terminal vibration control phase. The operator makes a second run to check the behavior with the vibration control in place. He may repeat the process after speeding up the robot motion along its trajectory if it is seen that the terminal vibration controller can handle larger vibrations. The robot is then ready for high speed operation.

THE CONTROL METHOD

The Identification Step

Consider the sensor requirements for the identification steps. Theoretically one may be able to perform the needed identification using only the sensors normally installed on a robot for feedback control. However, we want the identification to be quite accurate and to not require any sophistication in its use. For this reason, and for use in the feedback of the chosen vibration control method, it would be desirable that all system state variables be directly measured by sensors installed on the robot.

For a robot where the primary vibration source is from flexibility in belt drives, as is illustrated for two links in Fig. 1, the sensors needed consist of an angle encoder for the drive wheel and one for the driven wheel in each pulley system. Conceivably the velocities for each wheel could be obtained by taking differences of successive samples or could be obtained from feedback within the DC drive motors. Otherwise tachometer measurements would be needed for each. One of these angle encoders is automatically present on any robot for its own feedback control, so only one sensor per link need be added to the robot. On five or six axis robots the major sources of low frequency vibration will be in the first three arm links, with vibration from the wrist and hand often negligible. Hence, the number of extra sensors could be limited to three.

When the major source of vibrations is from harmonic drives instead of belts, the situation is essentially the same. However, because of the high ratios involved, it may be necessary to take some care in getting the required resolution on the output angle. This could be accomplished by using extra gearing introduced purely to run the encoder. Because the encoder is essentially a negligible load, it should be inexpensive to build an antibacklash system to maintain an accurate reading, or one could make use of another harmonic drive. One extra difficulty with harmonic drives is the

nonlinear spring constant behavior for very small angles which would not be modeled by a linear identifier.

The situation is more complicated when the major source of vibration comes from structural flexibility in the links. In this case sensors must indicate the amount of elastic deformation of each link. Strain gages mounted along the link is one imprecise method {1}. Various optical and laser methods are currently being studied by researchers, knowing that any sophisticated control of a flexible arm will require such measurements for feedback.

With the needed sensors in place, the identification test run performs the desired maneuver with the standard robot controller functioning, and without any attempt to suppress the resulting vibration. As discussed below, it will be necessary to momentarily interrupt the control signal with a control action unrelated to the current state in order to obtain full information. During the terminal phase of the test run, data is collected from the sensors and stored.

The robot microprocessor then uses the stored data to develop linear system equations appropriate for the present maneuver endpoint and the present loading and operating conditions. There are many choices for the identification method that develops these equations. One method that has recently proved very effective in the identification of vibrations in flexible structures is the Eigensystem Realization Algorithm ({}), which has a recursive form that is appropriate for PC type computers ({}). Here we adopt a more direct approach, one that may be as good as any when the full state is measured, and one which is quite simple to implement. We seek a system model of the form

$$x(k+1) = Ax(k) + Bu(k) ; \quad k = 0,1,2,\dots \quad (1)$$

where x is the $n \times 1$ state vector and u is the $m \times 1$ input vector. If the system state is measured for $N+1$ successive steps, then equation (1) written for each of the N values of k is

$$\begin{bmatrix} x(1) & x(2) & \dots & x(N) \end{bmatrix} = \begin{bmatrix} A & B \end{bmatrix} \begin{bmatrix} x(0) & x(1) & \dots & x(N-1) \\ u(0) & u(1) & \dots & u(N-1) \end{bmatrix} \quad (2)$$

If $N=n+m$ the matrix on the right can be inverted to solve for the system matrices A and B . Because of measurement noise, it would be advisable to use more data in the identification producing more equations than unknowns. Then, use of the Moore-Penrose pseudoinverse produces the desired identification

$$[A \ B] = [x(1) \ x(2) \ \dots \ x(N)] \begin{bmatrix} x(0) & x(1) & \dots & x(N-1) \\ u(0) & u(1) & \dots & u(N-1) \end{bmatrix}^+ \quad (3)$$

Note that the identification method will fail, as will all such methods, if $u(k)$ is a linear combination of $x(k)$ for all data points k taken. In this case one can only identify the corresponding linear combination of A and B that multiplies on the right of (1) when the control law is substituted. This difficulty applies, for example, when a classical proportional plus derivative controller is in operation, in which case it is necessary to override the controller with a different control signal for some data points in the identification test run. Note also that a priori knowledge of the presence of an eigenvalue at $+1$ has not been incorporated in the method. Such knowledge is generally very hard to incorporate in an identification process.

The computations required to evaluate equation (3) are simple enough that they can be done on a PC level computer. There are no computation time constraints since the identification is not being done on-line.

Terminal Deadbeat Control

Considerable progress has been made in recent years in deadbeat control theory, see for example References {4-10}. For the computations made in this study the deadbeat feedback control gains were computed using the formulas in (5). Methods exist that have better numerical properties, but no difficulties were encountered. The deadbeat gain matrix g^T in the control

$$u(k) = g^T x(k) \quad (4)$$

satisfies

$$g^T [A^1 B^{(1)} \ A^2 B^{(2)} \ \dots \ A^r B^{(r)}] = [-I_n \ 0_{r,n} \ \dots \ 0_r] \quad (5)$$

where the second matrix on the left side is an $n \times n$ full rank matrix obtained from the matrix

$$F_n = [A^1 B \ A^2 B \ \dots \ A^r B] \quad (6)$$

by deleting linearly dependent columns scanning the matrix starting from the left. Controllability is assumed and A is invertible so the matrix is full rank. The superscript on $B^{(1)}, \dots, B^{(r)}$ indicate the columns which remain in B for each power of A^i , the r_i are the number of remaining columns, and I_n is the

r, x, r , (i.e. the $m \times m$) identity matrix.

For certain computations open loop deadbeat control was computed, as well as a minimum norm control taking more than the minimum number of steps to get to the desired final state. This was accomplished by using equation (1) repeatedly to write $x(N)$ in terms of $x(0)$ and the control history to obtain

$$\begin{aligned} x(N) &= A^N x(0) + A^{N-1} B u(0) + \dots + A B u(N-2) + B u(N-1) \\ &= A^N [x(0) + F_N U(N)] \end{aligned} \quad (7)$$

$$U^T(N) = [u^T(0) \ u^T(1) \ \dots \ u^T(N-1)] \quad (8)$$

Then one form of the needed control sequence is written

$$U(N) = -F_N^+ [x(0) - A^N x(N)] \quad (9)$$

where F_N^+ is the Moore-Penrose pseudoinverse. When N is the minimum possible number of steps, this is the open loop deadbeat control sequence (and the pseudoinverse will reduce to a true inverse when $m=1$, and in some cases when $m>1$).

Saturation Considerations

A deadbeat controller is a controller that transfers the state to the desired state in a minimum number of steps. It does not acknowledge any control magnitude limitations that the hardware may have. Several options are at the disposal of the control system designer to prevent difficulty from control saturation.

First, the point at which the terminal vibration controller is turned on can be adjusted to prevent saturation problems. Second, the sample time can be adjusted. Since in a scalar control problem, the deadbeat control gets to the terminal state in n steps or less, increasing the discretization time step allows the control more time to accomplish its goal.

On the other hand, the derivation of the deadbeat control law suggests that perhaps the controller will still behave well in the presence of saturation. Consider the closed loop system matrix in the case of a scalar control $(A+Bg^T)$. This matrix has all zero eigenvalues with one true eigenvector

Any $x(0)$ can be written as a linear combination of the eigenvector and the generalized eigenvectors as

$$x(0) = \alpha_1 v_1 + \alpha_2 v_2 + \dots + \alpha_n v_n \quad (10)$$

Since $(A+Bg^T)v_1=0$, and $(A+Bg^T)v_{j+1}=v_j$, $j=1,2, \dots, n-1$, we see that in the first step of deadbeat control the component

of $x(0)$ on v_1 is annihilated, and the other components are transformed:

$$(A+Bg^T)x(0) = \alpha_2 v_1 + \alpha_3 v_2 + \dots + \alpha_n v_{n-1} \quad (11)$$

The second step annihilates the α_2 term of the $x(0)$ expansion, etc. This structure suggests that if the control action was insufficient to accomplish the annihilation of one of these components in one step, due to saturation limits, that it will finish the job in the next step, or the next few steps. In other words, it suggests that feedback deadbeat control in the presence of saturation will still give reasonable control commands, and the saturation simply causes the controller to take some extra steps to accomplish the aim. A better understanding of the degree to which this conjecture holds is obtained in the sequel.

One might hope that deadbeat feedback with saturation might in some way approximate true bounded time optimal control. Simple examples suggest that this approximation is not always good. The regions of the state space in which $u=+u_{\max}$ and $u=-u_{\max}$ for deadbeat control are bounded by two parallel straight lines

$$\begin{aligned} g^T x &= +u_{\max} \\ g^T x &= -u_{\max} \end{aligned} \quad (12)$$

These lines can be compared with the known continuous time, time optimal switching curves in simple examples where those curves are known such as the double integral plant and the harmonic oscillator. In the former case the switching structures are somewhat similar, but in the latter they seem to have little resemblance.

NUMERICAL RESULTS

Robot Models

Three robot models were used in numerical simulations. These were a single link arm model with structural flexibility, a single link with a flexible belt drive, and a two link arm with flexible belt drives. The last two models can also be considered to represent robots with harmonic drives, the main difference being the larger gear ratios obtained in these drives. There will be some inaccuracy involved because of the assumption of linear flexibility.

The modeling of the flexible arm was done in a very simple fashion. The kinetic and potential energies were taken to be

$$T = .5I\dot{\Theta}^2 + .5MR^2(\dot{\Theta} + \dot{\Psi})$$

$$V = .5KR^2\Psi^2 \quad (13)$$

where Θ is the undeformed or rigid body angle, and angle Ψ represents the deformation angle for the load end of the link. $I=0.09\text{kg}$ is the arm inertia, $R=0.3\text{m}$ its length from axis to load, and $M=0.1\text{kg}$ is the mass of the load. Note that the center of mass of the unloaded arm is assumed on the axis of rotation, and that the only kinetic energy of deformation included is associated with the load mass. The associated system equations are

$$\ddot{\Psi} + 2\xi\omega_n\dot{\Psi} + \omega_n^2\Psi = \frac{1}{I}u$$

$$\ddot{\Theta} - \frac{M}{I}r^2\omega_n^2\Psi - \frac{2\xi M}{I}r^2\omega_n\dot{\Psi} = \left(\frac{1}{I+MR^2} + \frac{M}{I}r^2\right)u \quad (14)$$

where damping has been included using a Rayleigh dissipation function with coefficient c , w is the applied torque at the base, and

$$\begin{aligned} M_o &= IM/(I+MR^2) \\ \omega_n^2 &= K/M \\ \xi &= (c/2)(1/KM_o)^{1/2} \end{aligned} \quad (15)$$

In computations $\xi=0$, and $\omega_n=2\pi(7/0.5)$ producing a period of $0.5/7$. A normalized time was used, normalized by the total time for the maneuver taken as $=0.5\text{sec}$, and the period in normalized time was $1/7$. The initial state was zero, and the final state zero except for Θ being 0.6313 rad. The state differential equations were discretized by use of a state transformation to Jordan form, computation of the matrix exponential in this form, and then transformation back.

The single link pulley model was obtained, again by use of Lagranges equations. Refer to Fig. 1 and consider that the base link is immobilized. Then the kinetic and potential energies are

$$T = 1/2I_3\dot{\Theta}_3 + 1/2I_4\dot{\Theta}_4 + 1/2m(r_L\dot{\Theta}_4)^2 \quad (16)$$

$$V = 2 \cdot 1/2K_2(r_3\Theta_3 - r_4\Theta_4)^2$$

Note that pretension in the belt need not be explicitly considered in forming V . Here I_3 is the inertia of the drive pulley and motor, I_4 is the inertia of the driven pulley and it's attached link (assumed for convenience to be statically balanced) and load, m is the mass of the load at distance r_L from the load pulley axis, and the angles and radii are as indicated in the figure. Values used are $I_3=1.0\text{kgm}^2$,

$I_1=0.7\text{kgm}^2$, $m=1.25\text{kgm}^2$, $r_1=0.8\text{m}$, $r_3=0.04\text{m}$, $r_4=0.08\text{m}$, $k_2=3.7\times 10^5 \text{ kg/sec}^2$, and the viscous damping coefficient for the belt $c_2=4700\text{kg/sec}$. The maximum torque level was set at 20 nt-m. After discretization with a time step of 0.01471 the resulting difference equation model (1) had the following system matrices

$$A = \begin{bmatrix} 0.8958 & 0.01350 & 0.2084 & 0.02411 \\ -12.194 & 0.8184 & 24.388 & 0.3612 \\ 0.1387 & 0.001605 & 0.7226 & 0.01150 \\ -16.237 & 0.2418 & -32.47 & 0.5164 \end{bmatrix}$$

$$B = [0.000103, 0.01305, 0.000007, 0.001605]^T$$

with the state variable being $x=[\theta_3, \theta_3, \theta_4, \theta_4]$.

The development of the two link robot equations started with the kinetic and potential energies

$$T = 1/2 I_1 \dot{\theta}_1^2 + 1/2 I_2 \dot{\theta}_2^2 + 1/2 I_3 (\dot{\theta}_2 + \dot{\theta}_3)^2 + 1/2 \bar{I}_4 (\dot{\theta}_2 + \dot{\theta}_4)^2 + 1/2 m \bar{l}_{24}^2 \dot{\theta}_2^2 + I_{4c} \dot{\theta}_4^2 + 2 \bar{l}_{24} I_{4c} \dot{\theta}_2 \dot{\theta}_4 \cos \theta_4 \quad (18)$$

$$V = K_1 (r_1 \theta_1 - r_2 \theta_2)^2 + K_2 (r_3 \theta_3 - r_4 \theta_4)^2$$

Here the I_1 and I_3 pulley inertias include the associated motor inertias, I_2 includes the inertia of the link joining pulleys 2 and 3, 4 with the link center of mass assumed on the pulley 2 axis for convenience, and I_4 is the inertia of pulley 4 together with its link and the load -- this time about the center of mass of this system whose mass is m and whose radial distance from the pulley 4 axis is l_{4c} . The final term of the kinetic energy expression is the translational energy for this center of mass. The \bar{l}_{24} is the distance from pulley 2 axis to pulley 4 axis. The resulting equations are of course highly nonlinear. They are linearized about the final desired state, and then discretized with a sample time of $T=0.03608$ for the computer runs. The details of the development are too complicated to report here. The parameters used included

$$\begin{aligned} I_1 &= 0.8\text{kg-m}, I_2 = 0.5\text{kg-m}, \\ I_3 &= 0.6\text{kg-m}, I_4 = 0.4\text{kg-m}, \\ m &= 2\text{kg}, \\ \bar{l}_{24} &= 0.6\text{m}, l_{4c} = 0.35\text{m}, \\ k_1 &= k_2 = 3.9 \times 10^5 \text{ kg/sec}^2 \\ r_1 &= r_3 = 0.04\text{m}, \\ r_2 &= r_4 = 0.08\text{m}, \end{aligned}$$

and the viscous damping coefficients for the Rayleigh dissipation function were $c_1 = 3800\text{kg/sec}$ and $c_2 = 3100\text{kg/sec}$. The maximum torque levels were set at 20nt-m for the base link, and 16 nt-m for the outer link.

Control Desaturation by Sample Time Adjustment

The robot models discussed above were used to study the usefulness of adjusting the sample time to reduce the maximum control effort requested by the deadbeat control commands. Certain of these results are cited in Table 1. The first entry uses the flexible robot model with time normalized by the terminal time $t_f=0.5$, and gives normalized controls $t_f^2 u/I$ where u is the applied torque. The maneuver used started at all zero initial conditions and applied a torque of $+2.78$ until $\tau=t/t_f=0.57$ at which time the torque was reversed to -2.78 until $\tau=0.71$ at which time the deadbeat vibration control was applied, with a target endpoint of $\Theta_f=0.6313$ rad with no deformation and no velocity. The initial condition for the deadbeat controller after the bang-bang control action, was $\Psi=d\Psi/d\tau=0$, $\Theta-\Theta_f=-0.0389$, and $d\Theta/d\tau=1.08$. Note that at this point the deformation Ψ and the deformation rate are zero. If one knows the system parameters well, one can usually adjust the bang-bang torque levels and the times in such a way as to have no residual oscillations. This approach to vibration suppression was studied with numerous examples, but was considered of limited value because of the sensitivity to the knowledge of the model and to implementation errors, and because of the difficulty of obtaining solutions in multiple link and hence multiple vibration frequency problems.

The second half of the table presents results using the two link pulley drive model. This time both torque motors were applied at their nominal maximum levels for $0 \leq t \leq 0.24$, and then reversed for $0.24 < t < 0.499$. The initial state chosen was

$$\begin{aligned} X(0) &= [\Theta_1, \dot{\Theta}_1, \Theta_2, \dot{\Theta}_2, \Theta_3, \dot{\Theta}_3, \Theta_4, \dot{\Theta}_4] \\ &= [0, 0, 0, 0, 0, 0, 0.474, 0, 0.237] \end{aligned}$$

The desired terminal state was $\Theta_1 = 2\Theta_2 = 0.46$ rad, $\Theta_3 = 2\Theta_4 = 1.006$ rad.

At the time the deadbeat control was turned on at $t=0.499$ sec the state error was

$$\begin{aligned} \Delta x &= [-2.18 \times 10^{-3}, 3.49 \times 10^{-4}, 1.79 \times 10^{-3}, -1.24 \times 10^{-3} \\ &\quad -1.12 \times 10^{-4}, -4.11 \times 10^{-4}, 8.86 \times 10^{-4}, -3.13 \times 10^{-3}] \end{aligned}$$

The general behavior observed in these results and others, is that for very small sample times compared to the period of oscillation in the system, doubling the sample time will reduce the control commands by approximately a factor of two. However, when the sample time nears one half the period of oscillation in

the system the maximum deadbeat control commands incurred goes through a minimum, and then it goes up dramatically as the sample time approached the period of oscillation. Thus there is a hard limit on the degree to which sample time adjustment can be used to satisfy control saturation limits in deadbeat control.

Table 1. The Deadbeat Control Sequence as a Function of Sample Time

Period of System Natural Frequency	Sample Time	Control Sequence			
1/7 = 0.143	0.08	-7.89	-10.63	-039	4.03
	0.1	-9.75	-0.823	-6.53	5.2
	0.1169	-29.79	41.9	-44.0	17.0
	0.1358	-290.9	721.5	-610.3	167.9
0.1, 0.1	0.02	99	-13	-286	200
		-67	20	145	-98
	0.04	-5.87	-6.48	27.5	-15.1
		-2.4	8.8	-14	7.7
	0.06	-39.9	76.4	-34	-2.65
		19.7	-40.3	19.9	1.0
	0.074	31.8	-58	20.7	4.81
		-17.7	31	-10.5	-2.43

Control Desaturation by Adjusting the Number of Time Steps Used

Deadbeat control gets the state to the desired state in a minimum number of steps which is less than or equal to the order of the system. It is logical to consider generating a control law that uses a prescribed number of steps which is larger than the minimum, in order to decrease the maximum torque commanded. Unfortunately, this is not currently a viable option in practice because of the lack of a feedback form for such a control law, but research is currently in progress on this issue. However, we do know how to generate an open loop form for such a control, and some computer runs using the flexible robot model were made to study this option. Starting from a rest position the maximum torque level was applied for $0 < t < 0.5$ and then reversed for $0.5 < t < 1.0$. If the arm were rigid, this would have resulted in a zero final velocity at the desired angle which we set to be zero by definition of the state variables. At $t=1$ the state is not zero, but rather

$$x(0) = [0.0014, 0.00015, -0.00013, -0.000014]^T$$

which is the initial condition for the vibration suppression controller.

Letting $x(N)=0$ in equation (7) produces the equation which

must be satisfied by the control sequence $U(N)$ in order to reach the origin in N steps. When N is greater than the number of steps used by deadbeat control, equation(7) has more unknowns than equations. The solution used in (9), with a Moore-Penrose pseudoinverse, gives the minimum norm solution for $U(N)$, and therefore should keep the maximum control small. Of course, one might improve upon this solution by looking for one that actually minimizes the maximum control.

Table 1 presents some results which combine adjusting the number of time steps used and adjusting the step size. First the number of time steps was picked, and then the step size was repeatedly adjusted until the maximum control effort encountered in the control sequence was roughly the same. This was found to be very sensitive in some cases. It is interesting to note that over the range of values studied the total time taken to accomplish the control objective was nearly invariant. This suggests that there is no point in adjusting the total number of time steps used unless one has already increased the size of the time steps to near the value which corresponds to the minimum control effort -- as discussed in the previous section.

Table 2. Desaturation by Increasing the Number of Steps

Period of System Natural Frequency	Number of Time Steps	Sample Control Period	Sequence	
1/7 = 0.143	4	0.024	0.21, 0.69, -2.01, 1.11	0.096
	5	0.018	-0.19, 1.54, -0.62, -2.63, 1.9	0.09
	7	0.014	0.38, 0.45, 0.014, -0.65, -1.04, -0.53, 1.38	0.098
	9	0.01	-0.38, 0.81, 1.05, 0.48, -0.58 -1.59, -1.85, -0.64, 2.7	0.09

Deadbeat Control of One and Two Link Belt Drive Robots

Figures 2 and 3 show the simulation results for using deadbeat control on the belt drive robot models described above. Figure 2 applies to the single link problem. The bang-bang torque history shown for $0 \leq t \leq 0.5$ sec is such that it would transfer the arm to the desired position at 0.5 sec. When applied with the pulley system, vibrations are excited. The second curve in the figure represents $(r_3/r_4)\Theta_3 - \Theta_4$, which would be zero at all times if the belt did not stretch, and hence indicates the amount of vibration. At $t = 0.5$ the deadbeat control is turned on and the oscillations killed in 4 steps, or approximately 0.06 sec. The dashed curved indicates the free decay of oscillations (with the chosen damping ratio which is

-0.3) for comparison.

Figure 3 shows the results of a complete simulation of the proposed identification and control method on a two link, 2 pulley, nonlinear robot system. The parameters for the computer run were described in the discussion of Table 1 and in the description of the model. The first part of the figure shows the torque on the base link and the base link vibrations $(r_1/r_2)\Theta_1-\Theta_2$, and the second half shows the corresponding quantities for the second link. The output of the simulation of the nonlinear equations was used in the identification package to obtain the A and B matrices, and the deadbeat feedback gains. Then a second simulation applied these gains starting at $t = 0.5$ to kill the oscillations, as shown in Fig. 3.

In order to study the effects of noise in the data, other computer runs were made in which the A and B matrices had components which were arbitrarily changed by 10%. The deadbeat control for these incorrect system matrices was applied and found to behave well. The price that was paid was an increase in the number of steps before the final state was reached, which in some cases took an extra 6 steps to kill the error. Hence, the feedback form being used can account for modelling errors.

These simulations show the potential of the proposed vibration control concept, and show that for the system models considered the method works very well.

EXPERIMENTS

In order to study in more detail the promise and limitations of the proposed robot control method, an experimental set-up was developed that is typical of a certain class of robots having belt drives on each of the axes. The needed software was developed and then applied, to perform the identification step from data taken on a test run, to obtain the deadbeat feedback gains from the identification results, and then to apply the deadbeat control to the hardware. In order to understand the results of the experiments, various simulation studies and analytical studies were also performed.

Apparatus

Attention was focused on the control of one joint of a robot. The base drive of an industrial electrically driven robot, the Systems Control Model 751, was used. This drive is a DC motor with a built-in gear ration of 5.5:1, using typical industrial gearing. The motor was used to drive the load through a 3 to 1 pulley system as is done on the base joint of the 751, but a larger pulley was substituted that is more typical of other axes of this robot. Instead of using the robot

itself as the load on the motor and somehow freezing the other axes for the experiment, a different inertial load was substituted in the form of a dumbbell consisting of disks of mass 10 lb. at each end of a rod of length 10 in., which was turned in the horizontal plane about its center.

Optical shaft encoders manufactured by Teledyne Gurley were placed on each of the pulleys. The encoders had a net resolution of 86,400 pulses/revolution. The motor driving the system was a standard gearhead motor from Bodine Electric Corp. It was rated at 110 V., 1A and 1/8 H.P. Backlash in the gearhead was measured at about .5 degrees. The motor was driven by a Motion Sciences amplifier which was rated at 4A/50V. The amplifier was supplied a $\pm 5V$ analog signal from a D/A board with 12 bit resolution. Thus the analog voltage resolution was $10/4096 = 2.4mV$. The board was a plug in card in a 10MHZ IBM-AT clone fitted with an 80287 math coprocessor.

The optical encoder signals were processed by an HP2000 based circuit. These circuits took the two quadrature signals from each encoder and translated them into positive or negative counts. The HP2000 circuits had a 12 bit internal counters which were read by the computer through a digital 8 bit parallel port. Since the counters were limited to 12 bits, they were read at least once every 50m sec. (maximum interval between successive reads) to ensure that counts would not be lost due to overflow or underflow.

The input and outputs were processed on the AT-clone using interrupt driven code. The software was written in Turbo Pascal. The speed of the AT-clone combined with the compiler allowed the interrupt time to be set to any value between .5m sec.-50m sec.

The Identification Step

The first step in the proposed control procedure is to perform a test during which data is taken, and then obtain a system model from the data. The state variables for the difference equation model included the motor angle x_1 , and the inertial load angle x_2 . Since no direct measurement of velocity was made, x_3 and x_4 were the differences between current values of x_1 and x_2 respectively, and their values at the previous sample time. The DC motor was considered fast enough that there was no need for any motor state, and hence the fourth order model represented rigid body rotation and belt vibration.

For later comparison purposes, a proportional plus derivative (PD) controller was generated and tuned to give good performance. A gain of 0.5 on motor position feedback and of 3 on the motor "velocity" x_3 was used when a sample time of 5

milliseconds was employed, and this gave slightly underdamped response.

The identification test data was obtained with this controller in operation. However, if the controller is on for all time steps of data taken, the control actions will be a linear combination of the state. This means that the matrix on the right of equation (2) is not full rank, and one cannot complete the identification. As a result, the PD controller was interrupted with an arbitrarily chosen control action for several time steps during each test.

Figures 4 to 7 give typical test results. In this particular run, a torque level of -448 units (where -2048 units is maximum torque) was applied for a short time (roughly 10 secs. seconds), immediately after which the encoder counters were set to zero and data was taken for the next 41 time steps of 5 milliseconds. During this time the control action was switched to +448 counts for the first six steps, and then the PD controller was applied. The PD control law was made to aim at $x_1=9000$ and $x_2=3000$ counts by subtracting these numbers from the states used in computing the control. Setting the encoders to zero as above, assumes that the belt is not significantly stretched at the time. This appears not to be a problem, since similar results were obtained starting from zero velocity.

The first of the 41 data points does not give x_3 and x_4 since these are changes in x_1 and x_2 from the previous step. The remaining 40 data points were used to obtain the A and B matrices according to equation (3) and resulted in

$$A = \begin{bmatrix} .9239 & .2432 & .8841 & .1066 \\ .0018 & .9949 & -.0002 & .9904 \\ -.0761 & .2432 & .8841 & .1066 \\ .0081 & -.0051 & -.0002 & .9904 \end{bmatrix} \quad (19)$$

$$B^T = \begin{bmatrix} -.0371 & -.0051 & -.0002 & -.9904 \end{bmatrix}$$

The eigenvalues of A are

$$\lambda(A) = .9700, 1.0153, .9040, .2681i$$

The first two represent the rigid body mode which would both lie precisely at 1.0 if there were no damping in the system and the data was perfect. The complex conjugate pair represents the belt vibration which corresponds to a lightly damped oscillation of period 0.11 seconds. This period is typical of robot vibrations.

As a test on the identification results, the states

specified by the data at the second time step in the sequence of 41 steps were used as initial conditions for the model (1, 19). The 40 time step state history predicted by the model and the 40 time steps of data recorded are both shown in Figs. 4 to 7. The inertial load position is perhaps the most important of the state variables since it is the actual variable to be controlled. Figure 4 shows excellent agreement between model and data. The velocity of the inertial load is represented by a difference between successive positions and is therefore somewhat noisier, but it is also seen to be in good agreement in Fig. 5. The motor position and motor velocity comparisons are given in Figs. 6 and 7. Only the motor velocity curve shows substantial differences, which might be attributed to backlash in the gears on the motor that is a nonlinear phenomenon the identification cannot model.

We conclude that the identification method is practical, can be done on a PC class computer (an IBM AT was used), and gives results which are sufficiently reproducible for the applications considered. The only trouble encountered was that occasionally some data points would appear that were clearly spurious, which would then give poor results. In this case we simply re-ran the identification test. But with small modifications to the identification program one could make it possible to skip data points when desired.

Deadbeat Control Experiments

Given the A and B matrices identified above, the deadbeat feedback gains were obtained on the IBM AT computer, which was then used to compute the control commands in real time and send them to the current driver for the DC motor. The deadbeat feedback control law obtained for the identification test described above, was

$$u(kt) = g^T x(kt) \quad (20)$$

$$g^T = [-104.7 \quad 8942.0 \quad -184.5 \quad 12760.4]$$

That these gains do in fact give deadbeat control, is established by computing the eigenvalues

$$\lambda(A - Bg^T) = -0.0451 \pm 0.0481i; +0.0451 \pm 0.0425i$$

which are as close to zero as one might expect, considering the difficulty of getting accurate roots in a matrix nominally having four identical eigenvalues in a Jordan form. A second check is made by simulating the application of this control to the system model. This completes the control objective in 4 steps, with a small 5th step residual control action to handle small numerical inaccuracies.

Many different experiments were run varying the possible parameters. Some experiments started with an initial velocity and aimed for specific counter readings, in the same manner as described above for the specific identification test discussed. This type of experiment is most representative of the robot applications envisioned, since the deadbeat control would be turned on as the arm approaches the end point. Other experiments went from a position with zero velocity, to another position with zero velocity. Thus the experiments varied the total distance travelled and the initial velocity.

The identification and feedback gain computations were repeated under these different conditions, and found to give reasonably consistent results. For example, when the identification test described in the previous section was repeated with zero initial velocity and an aim point of 3000 and 1000, the feedback gains obtained were

$$g^T = [-113.5 \quad 5728.3 \quad -308.4 \quad 10428.6]$$

Also, because the identified system never has an eigenvalue precisely at +1 as it should to allow a pure rotation of the two pulleys, two methods of indicating the counter aim points were compared. The first does the identification as previously described and inserts the aim point by applying

$$u(kt) = g^T [x(kt) - x_0]$$

The second subtracts x_0 from the encoder data before performing the identification, and then applies $u = g^T x$. Simulation studies showed negligible difference between these two approaches.

The results for all tests were similar. Typical results are shown in Figs. 8 and 9 which apply to a commanded change of 3000 motor encoder units and 1000 inertial load encoder units from a current rest position. Figures 8a and 8b show for comparison purposes the motor encoder angle and the control command as a function of time step, for the proportional plus derivative controller which is seen to give somewhat underdamped behavior. Figures 9a and 9b give the corresponding results for the deadbeat control law. It is seen that the deadbeat control gets the motor position into the neighborhood of the desired position much quicker than the underdamped PD controller, but that the system then goes into a complicated oscillation which does not decay. The next sections describe the studies made to understand this unacceptable behavior.

The Control Saturation Nonlinearity

The list of potential causes of the observed oscillation would include effects such as backlash in the gears, stiction, and limits on the possible control effort. A backlash of 0.5 degrees, for example, would seem reasonable in this system, and at approximately 86,400 counts per revolution this is equivalent to approximately 125 counts. Such a magnitude is consistent with Fig. 7 if backlash is the explanation of the differences between the observed and modelled curves. To study stiction the steady state velocity observed was plotted against constant discrete torque command levels in Fig. 10. This indicates that the command had to reach roughly 350 units out of its maximum level of 2048 before any motion was observed, and that above a command of approximately 1300 units no further increase in velocity is observed, suggesting that the actual torque saturation limit is 1300 units. Another way to observe the stiction effect is that a command to move from rest at the present position to rest at a position 120 units away, produces no motion when applying the PD control law.

Although backlash and stiction nonlinearities are clearly possible causes, attention was directed to the control saturation nonlinearity because the saturation level was so extremely low compared with the control commands generated. Certain simulation results illustrate this. Consider the 0.5 millisecond sample time that applies to all the results we have cited. Although it is clearly impossible in practice, on a computer one can ask for a change of 0.3 counter units of the motor angle, and 0.1 counter units of load inertia angle. For this case, the deadbeat control actions do not go above the 2048 saturation limit. However, if a change of 3 and 1 counter units is requested then the control actions encounter saturation. This one counter unit change in the inertial load angle corresponds roughly to 0.004 degrees.

In order to study the control saturations influence on the system behavior, a series of simulations were made in which the saturation limit was decreased in stages. We consider commanding a change from the current rest position to a neighboring rest position 30 motor and 10 load counter units away. Note that this distance is still too small to be physically realizable in the presence of stiction and backlash.

When there is no saturation limit, the maximum deadbeat control command encountered was 241,001 units compared to the 2048 limit, and the requested position was essentially reached in 4 steps, with a small residual annihilated on the 5th step. As expected, when we started to impose saturation limits the system still worked well, but took a little longer to reach the endpoint. For example, with a maximum control limit of 240,000,

the endpoint was reached in 5 steps, which was also true at 230,000. A control limit of 200,000 caused the system to require about 7 steps, at 190,000 it was up to 9 steps and at 184,000 it took 14 steps. Such behavior is consistent with our expectation that deadbeat control might still work well when its commands are limited by hardware saturation.

However, when the saturation limit was decreased still further a striking event occurred. When the limit was decreased from 184,000 to 183,550, the number of steps required went from 14 to infinity. At 183,550 the system went into perpetual high amplitude oscillations. A further decrease of the saturation limit to 150,000 produced the same type of behavior with close to the same amplitudes and frequencies. These results are illustrated in Figs 11 through 14. In making comparisons, note that the scales used are not always consistent.

The observed sudden onset of oscillations suggests a limit cycle induced by the saturation nonlinearity. The computer simulations used the linear model from the identification step, and predicted that the system would fail to work properly if the actual control saturation limits were imposed. Other nonlinearities like backlash and stiction might compound the situation, but are not needed to predict unacceptable behavior. It is perhaps unfair to compare the amplitudes of the oscillations observed in hardware, with the much larger amplitudes in the figures that correspond to much larger saturation limits, but it is conceivable that stiction effects actually decrease the amplitude of the limit cycle observed.

Among the methods suggested previously to desaturate the control action is to adjust the sample time used. Various sample times were tried. With the identified system natural frequency having a period of 0.11 seconds, clearly the sample time could be increased from .005 seconds to perhaps .02 seconds and still maintain reasonable discrete modelling of the continuous system dynamics. An increase in sample time by a factor of 4 would decrease the deadbeat command levels by approximately a factor of 4. This number is far too small to desaturate the control, since even for the unrealistically small 10 inertial load counter units commanded in the above series of simulation, the maximum control was a factor of approximately 120 times the nominal saturation limit.

We conclude that the observed unacceptable behavior of the deadbeat control system is due to the onset of a limit cycle caused by the saturation limit, and that the methods currently available to avoid saturation are insufficient for the task for the type of system being tested. The expectation stated earlier, that bounding the deadbeat commands should produce a well behaved but somewhat slower acting control, were seen to be

true-up to a point. And beyond that point the limit cycle takes over. The next section develops analytical methods to predict where that point occurs.

Limit Cycle Analysis

Methods are developed in this section using a describing function approach to predict the saturation limit at which limit cycle behavior starts in a system employing deadbeat control. The describing function analysis is necessarily somewhat unusual because the system model is in discrete form rather than a continuous time differential equation, and because it is in modern state variable form involving full state feedback, rather than the usual classical control system feedback. The equations are then:

$$\begin{aligned} x(k+1) &= Ax(k) + Bu(k) \\ u(k) &= \text{sat}[g^T x(k)] \end{aligned} \quad (21)$$

where A and B come from the identification, g is the deadbeat feedback gain, and sat(.) is a saturation function with unit gain up to its maximum output denoted by S.

The basic assumption of a describing function analysis is that the input to the nonlinear element is purely sinusoidal, with the harmonics generated by the nonlinearity being filtered out by the system model so that they have negligible amplitude when the signal gets back to the nonlinearity. Thus we assume that $g^T x(k)$ is a sampled sinusoidal signal, apply the saturation to it, obtain the amplitude of the fundamental in the Fourier expansion of the output of the saturation element, and denote the ratio of output fundamental amplitude to input amplitude M by DF(M), the describing function:

$$g^T x(k) = M \sin(\omega k T + \phi) \quad (22)$$

$$\text{sat}(g^T x(k)) = (DF) M \sin(xkT + \phi) \quad (23)$$

$$DF(M) = \begin{cases} \frac{2}{\pi} \left[\sin^{-1}\left(\frac{S}{M}\right) + \frac{S}{M} \sqrt{1 - \left(\frac{S}{M}\right)^2} \right] & \text{for } M > S \\ 1 & \text{for } M \leq S \end{cases} \quad (24)$$

The describing function is plotted in Fig. 15 [11,12].

With equation (23) as the driving function in (21) we need to solve this difference equation for $x(k)$. This is easiest done by replacing the sine by an exponential, finding the solution, and then taking the imaginary part. Then

$$x(kh) = Ax(k) + b(DF) M e^{j(\omega k T + \phi)} \quad (25)$$

and we substitute a solution of the form

$$x(k) = ve^{i\omega kT} \quad (26)$$

to obtain

$$v = (Ie^{i\omega T} - A)^{-1}b = (DF)Me^{i\phi} \quad (27)$$

To complete the feedback loop, the $g^T x_k$ associated with this solution must equal the assumed sinusoidal input

$$g^T x_k = g^T v e^{i\omega kT} = M e^{i(\omega kT + \phi)} \quad (28)$$

Substituting equation (27) gives

$$g^T (Ie^{i\omega T} - A)^{-1}b = 1/DF(M)$$

which is the fundamental equation determining whether a limit cycle can exist in the system. We need to determine whether there is a real positive frequency and a real positive amplitude which satisfies this equation, where $DF(M)$ is given in equation (24).

Several transformations are needed to facilitate this determination. Because of the discrete nature of the problem, write $z = \exp(i\omega T)$. Frequency response in the z plane is easiest done by further transforming to the w plane, and substituting a purely imaginary $w = i\omega_n$ [13]. Then the relationship between the true frequency ω and the new frequency variable ω_n is given

$$z = \frac{1+w}{1-w} = \frac{1+i\omega_n}{1-i\omega_n} = e^{i\omega T} \quad (30)$$

$$\omega = \frac{1}{T} \arctan 2(2\omega_n, 1-\omega_n^2)$$

In terms of the variable z , the left hand side of (29) can be evaluated as follows {14}

$$g^T (Iz - A)^{-1}b = \frac{z^3(g^T B_0 b) + z^2(g^T B_1 b) + z(g^T B_2 b) + (g^T B_3 b)}{z^4 + d_1 z^3 + d_2 z^2 + d_3 z + d_4}$$

$$= \frac{N(\omega_n)}{D(\omega_n)}$$

$$\begin{aligned} B_0 &= I & d_1 &= -\text{tr } A \\ B_1 &= A + d_1 I & d_2 &= -\frac{1}{2} \text{tr } AB_1 \\ B_2 &= AB_1 + d_2 I & d_3 &= -\frac{1}{3} \text{tr } AB_2 \\ B_3 &= AB_2 + d_3 I & d_4 &= -\frac{1}{4} \text{tr } AB_3 \end{aligned}$$

$$N(\omega_n) = (1-i\omega_n)(1+i\omega_n)^3(g^T B_1 b) = (1-i\omega_n)^2(1+i\omega_n)^2(g^T B_1 b) \\ + (1-i\omega_n)^3(1+i\omega_n)(g^T B_2 b) + (1-i\omega_n)^4(g^T B_3 b)$$

$$D(\omega_n) = (1+i\omega_n)^4 + d_1(1-i\omega_n)(1+i\omega_n)^3 + d_2(1-i\omega_n)^2(1+i\omega_n)^2 \\ = d_3(1-i\omega_n)^3(1+i\omega_n) + d_4(1-i\omega_n)^4$$

Combining the above results, we can rewrite the fundamental equation (29) in terms of ω_n as follows:

$$\text{Im}\{g^T [I(\frac{1+i\omega_n}{1-i\omega_n}) - A]^{-1} b\} = 0$$

or

$$F(\omega_n) = \text{Re}D(\omega_n)\text{Im}N(\omega_n) - \text{Im}D(\omega_n)\text{Re}N(\omega_n) = 0$$

and the real part is

$$\text{Re}\{g^T [I(\frac{1+i\omega_n}{1-i\omega_n}) - A]^{-1} b\} = 1/DF(M)$$

or

$$DF(M) = \frac{[\text{Re}D(\omega_n)]^2 + [\text{Im}D(\omega_n)]^2}{\text{Re}N(\omega_n)\text{Re}D(\omega_n) + \text{Im}N(\omega_n)\text{Im}D(\omega_n)}$$

The procedure to determine if there exists a frequency ω and amplitude M satisfying equation (29) is then to solve equation (32) for ω_n by plotting (Fig. 16), substitute this ω_n into equation (33) to find DF , and use this DF in Fig. 15 to obtain the limit cycle amplitude M . The actual limit cycle frequency ω is obtained from ω_n using equation (30).

Applying this procedure to the identified system model with the actual torque saturation limits resulted in a predicted limit cycle. This establishes that deadbeat feedback control can produce unacceptable behavior when control saturation is present. The limit cycle period predicted was significantly shorter than the observed period in simulation. It is presumed that higher frequency terms may play a significant part in the observed limit cycle, because the torque signals are essentially always in saturation producing sizable high frequency components, and because the system can fail to effectively filter some of these components, contrary to the assumptions of the describing function analysis, partly because the state feedback includes velocity feedback variables.

SUMMARY AND CONCLUSIONS

The primary limitation encountered in trying to increase the operating speeds of robots, and hence increase robot productivity, is the mechanical vibrations that are excited by the high accelerations and decelerations. The research reported here studies the problem of actively controlling these vibrations in order to allow higher operating speeds. The approach taken has three important properties:

1. The approach solves the difficulty of finding control design methods for the highly nonlinear robot dynamic equations, by choosing to control the vibrations as the robot approaches its desired end position. This allows the use of a linear model and hence the vast body of linear control theory can be applied to the problem. (It also means that in the future when time optimal control for robot motions {15,16} nears the application stage, the time optimal control computations can use rigid body models without modelling vibration sources--a vast simplification. If the vibrations can be killed by the terminal controller, one need not fear exciting them)

2. The approach solves the problem of obtaining a good dynamic model of the system in all possible configurations and load conditions, for purposes of control law development, by requiring the robot operator to perform a test run during which data is automatically taken and stored. It is then used by the robot microprocessor to develop the needed model.

3. The approach chooses to use deadbeat control to kill the oscillations, because deadbeat control is time optimal for a discrete model, and because a feedback form of the control law is available.

The simulation and experimental experience gained in this research leads us to the following conclusions.

Item 1 above seems to be a very smart way to go. The limitation to its application is that the vibrations must be due to approximately linear phenomena when near the end position -- such as vibrations due to the use of belt drives, or harmonic drives, or due to structural flexibility. Backlash and stiction must not be dominant.

Item 2 above also appears to be quite promising. System identification can be a somewhat tricky field, but the

straightforward approach adopted here gave good results, and appeared to be something which could be performed in an automatic manner by a robot operator who has no expertise in the control field. It can also be performed on in PC level microprocessor so that for many robots, no extra computation power is needed. It does require extra instrumentation of the robot, but this is perhaps limited to as few as three extra sensors. Obtaining the state variables by differencing the position measurements worked in the experiments so one need not use sensors for their direct measurement. The required sensors can be standard off the shelf items when the main source of vibrations is from belt drives. Some extra gearing might have to be designed in the case when harmonic drives are the major source of vibrations, but this is a simple matter. When structural flexibility is the main source, there is a need for novel sensor designs, and this is currently being studied by various research groups for use in control. The main difficulty encountered in the automatic use of the identification package was that occasionally there would appear a totally spurious data point which would disturb the identification. These were obvious when graphs of the data were displayed on the monitor. With different hardware, this might not be a problem. Otherwise, some procedure needs to be used to either eliminate such data points, or rerun the test.

The choice of deadbeat control as the control law in Item 3 above was the problematic step. It was seen to work well in simulations, but failed when applied to the specific test hardware. Hence, use of deadbeat control should work well for some class of robot problems, such as ones with very low frequency vibrations and powerful drive systems, but not for the range of parameters that is perhaps most typical of current robot designs.

The main difficulty in the success of deadbeat control is the actuator saturation level in applying the control commands. The following approaches to the saturation question were discussed with the following conclusions:

1. It was suggested, based on the theory underlying feedback deadbeat control, that the control might work well even with saturation present, since the saturated feedback actions would still be moving in the right direction. This statement was shown to be right -- but only up to a point. If pushed too far, the saturation nonlinearity was seen to introduce a limit cycle in the experiments. A method of analysis was developed to predict how small the saturation limit can be and still expect good behavior from a deadbeat feedback controller.

2. As the robot nears the desired endpoint, the time at

which the deadbeat control is activated can be used as a parameter to adjust to avoid saturation problems. In some applications, this parameter is surely a powerful tool to accomplish the aim. However, for the experimental hardware tested, this parameter was insufficient for the task. It would force the point of activation to be so late in the trajectory that it served

no real purpose to turn on the deadbeat control.

3. The digital sample time used in the data generation and system model can be adjusted to help handle saturation problems. Simulation results show that increasing the sample time generally decreases the maximum control action, but only until the sample time reaches the neighborhood of one half the period of the system frequency. For the parameters of the experimental test equipment, this limitation was too severe to allow desaturation by this approach.

We conclude that the overall approach taken is quite viable, and holds considerable promise for significantly increasing robot operating speeds. However, to accomplish this, improved digital control law design methods will be needed, that can transfer the state to the endpoint in minimum time, or near minimum time, in the presence of saturation limits on control effort. This requires extension of the current control theory, and the authors are currently conducting research in this area.

REFERENCES

1. J.N. Juang, L.G. Horta, H.H. Robertshaw, "A Slewing Control Experiment for Flexible Structures," Journal of Guidance, Control and Dynamics, Vol. 9, No. 5, Sept.-Oct. 1986, pp. 599-607.
2. R.W. Longman, and J.N. Juang, "A Variance Based Confidence Criterion for ERA Identified Model Parameters," Proceedings of the AAS/AIAA Astrodynamics Specialist Conference, Advances in the Astronautical Sciences, Kalispell, Montana. To appear
3. R.W. Longman, and J.N. Juang, "A Recursive Form of the Eigensystem Realization Algorithm for System Identification," Journal of Guidance, Control, and Dynamics to appear.
4. J.A. Cadzow and H.R. Martins, Discrete-Time and Computer Control Systems, Prentice-Hall, Englewood Cliffs, N.J., 1970.
5. B. Leden, "Multivariable Dead-Beat Control," Automatica, Vol. 13, 1977, pp. 185-188.
6. F. Kucera, "The Structure and Properties of Time-Optimal Discrete Linear Control," IEEE Transactions on Automatic Control, Aug. 1971, pp. 375-377.
7. B.C. Moore, "On the Flexibility Offered by State Feedback in Multivariable Systems Beyond Closed Loop Eigenvalue Assignment," IEEE Transactions on Automatic Control, Vol. AC- , Oct. 1976, pp. 689-692.
8. G. Klein, and B.C. Moore, "Eigenvalue-Generalized Eigenvector Assignment with State Feedback," IEEE Transactions on Automatic Control, Vol. AC-Feb. 1977, pp. 140-141.
9. G. Klein, "On the Relationship between Controllability Indices, Eigenvector Assignment, and Deadbeat Control," IEEE Transactions on Automatic Control, Vol. AC-29, No. 1, Jan. 1984, pp. 77-79.
10. G. Klein, "The Structure and Freedom in Selecting Deadbeat Controllers,"
11. Y. Takahashi, M. Rabins, and D. Auslander, Control and Dynamic Systems, Addison-Wesley Publishing company, Reading, Massachusetts 1970, pp. 523-525.
12. K. Ogata, Modern Control Engineering, Prentice-Hall Inc., Englewood Cliffs, N.J., 1970, pp. 538-551.
13. B. Kuo, Digital Control, McGraw Hill, New York, 1977.
14. T.E. Fortmann, and K. Hitz, An Introduction to Linear Control Systems, Marcel Dekker, New York, 1977.
15. J.E. Bobrow, S. Dubowksy, and J.S. Gibson, 'Time Optimal

Int. J. of Robotics Research, Vol. 4, No. 3, Fall
1985.

ASME Transactions, Journal of Dynamic Systems, Measurement and
Control, Vol. No. , 1979 , pp.

16. H.G. Bock and R.W. Longman, "Time Optimal Robot
Maneuvers," to appear.

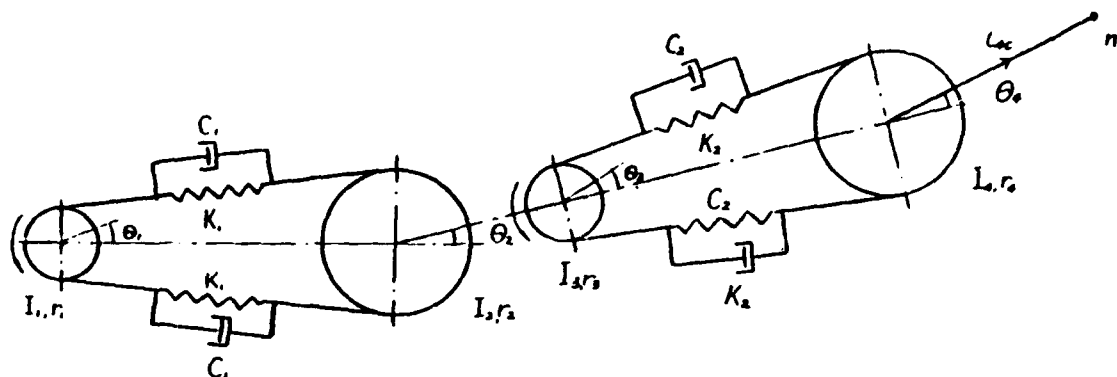


FIG 1 TWO LINK BELT DRIVE ROBOT MODEL

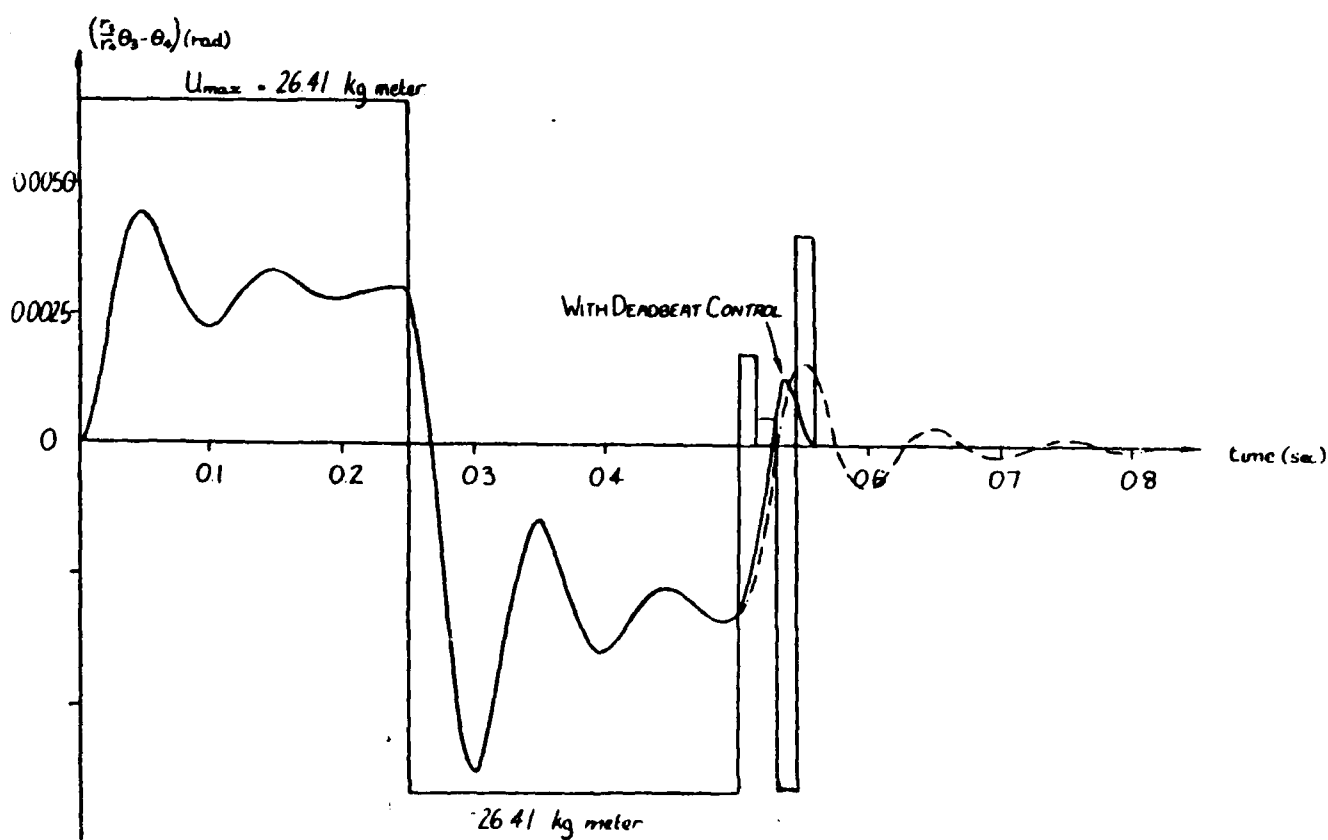


FIG 2 SINGLE LINK BELT DRIVE SIMULATION

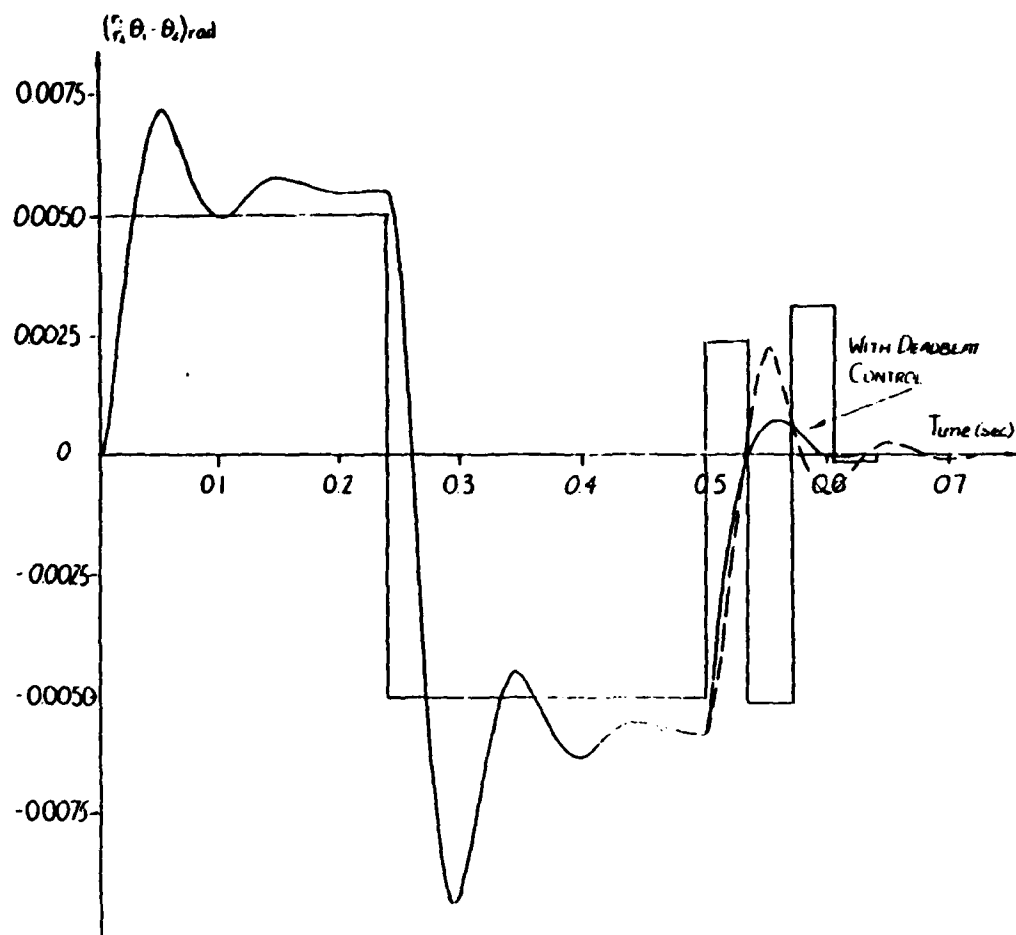


FIG 3a. INNER LINK. BELT DRIVE SIMULATION (TWO LINK)

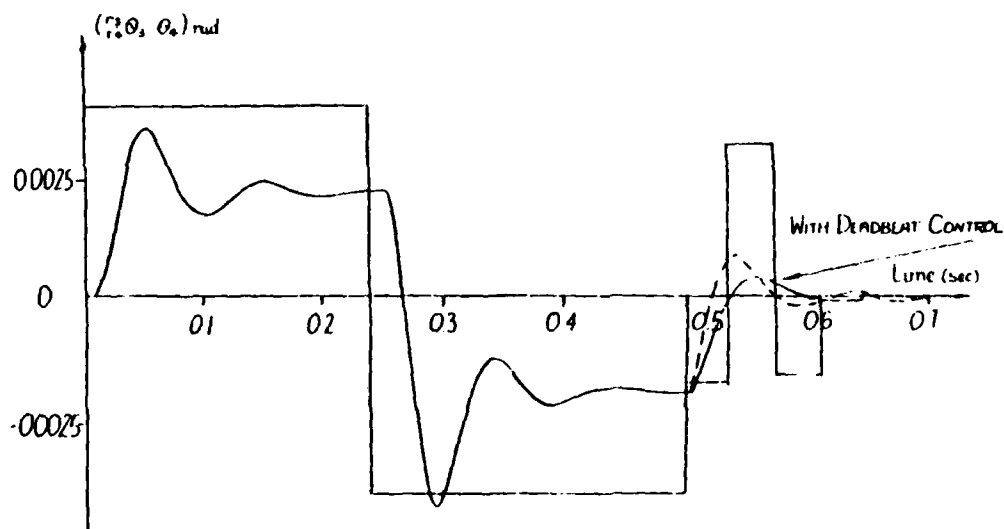


FIG 3b. OUTER LINK. BELT DRIVE SIMULATION (TWO LINK)

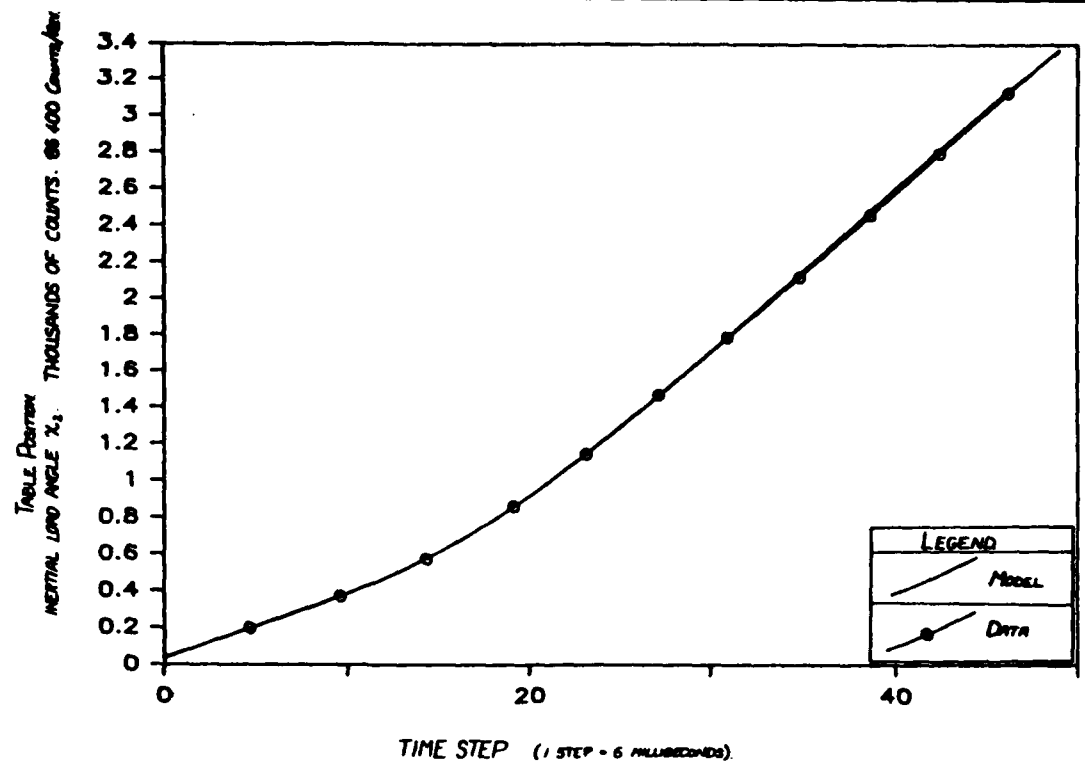


FIGURE 4 Comparison of Model and Data: Inertial Load Angle

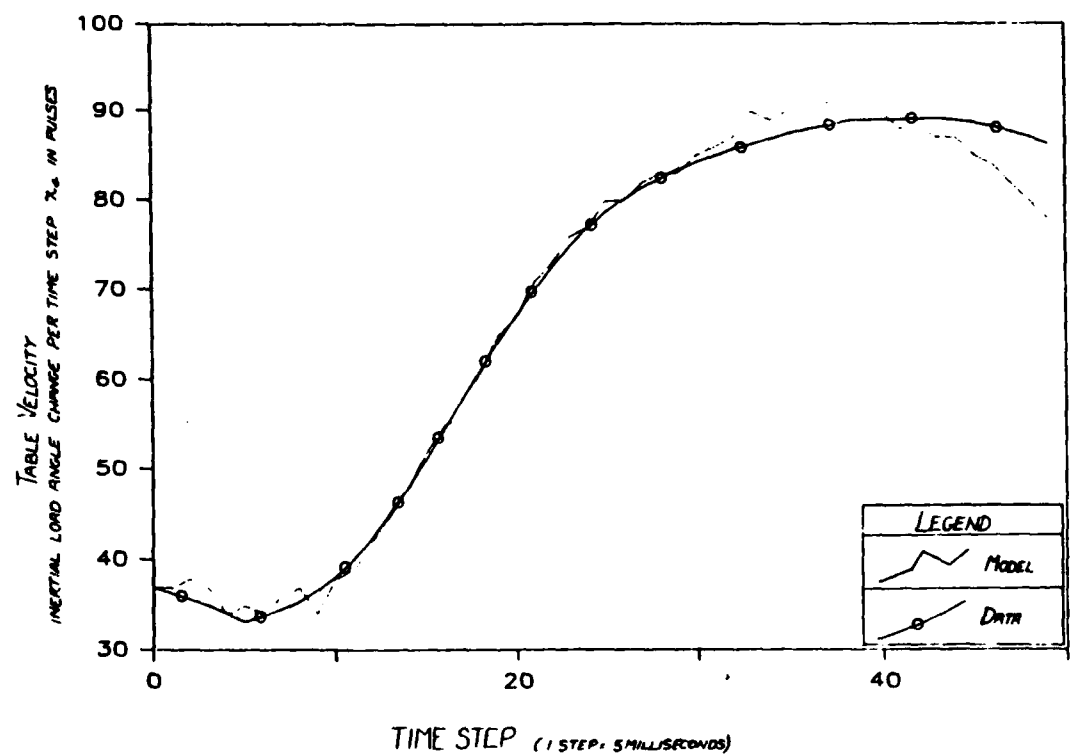


FIGURE 5 Comparison of Model and Data: Inertial Load Velocity

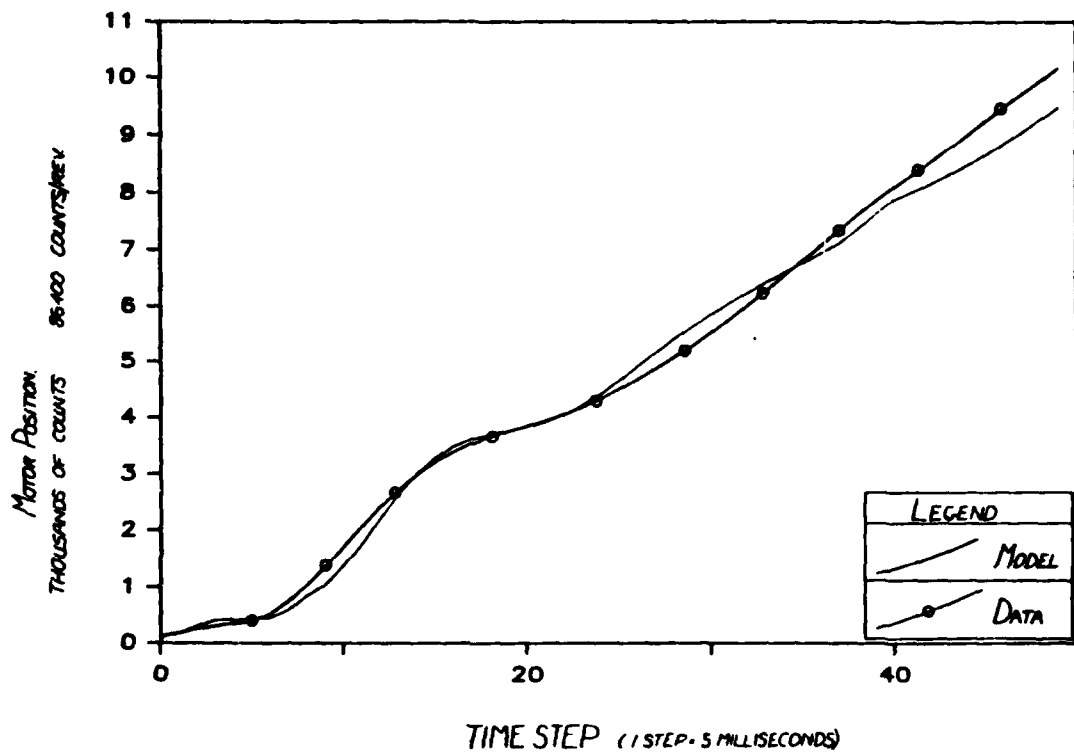


FIGURE 6 Comparison of Model and Data: Motor Angle

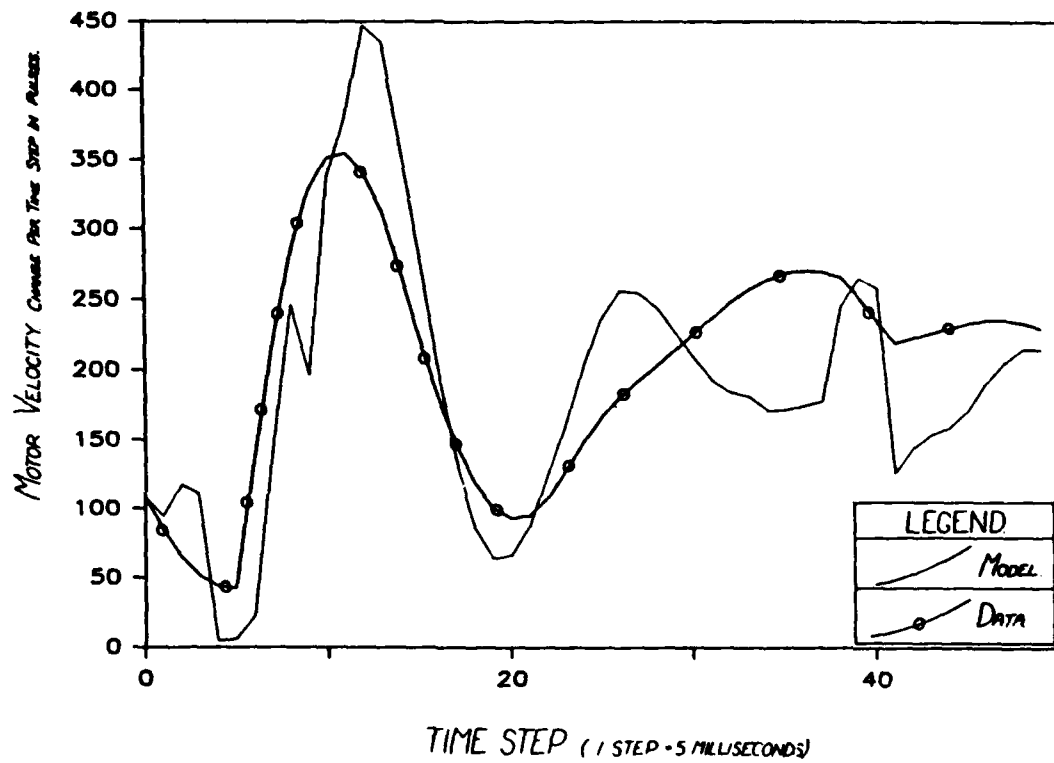


FIGURE 7 Comparison of Model and Data: Motor Velocity

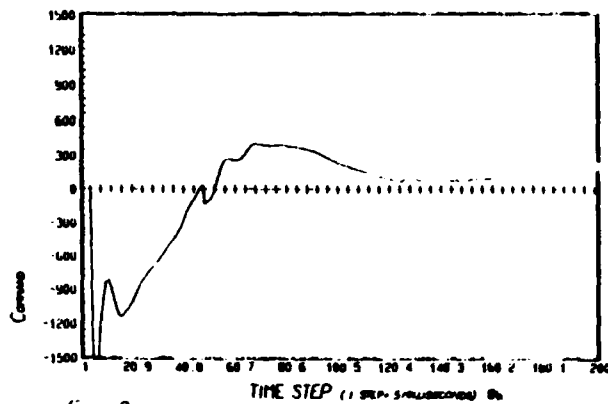
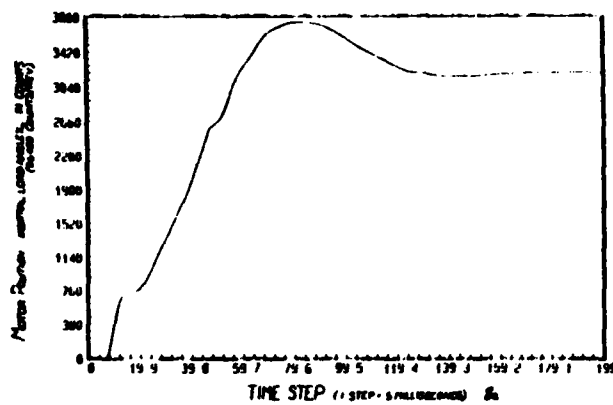


FIGURE 8 Experimental Motor Position and Command for PD Control

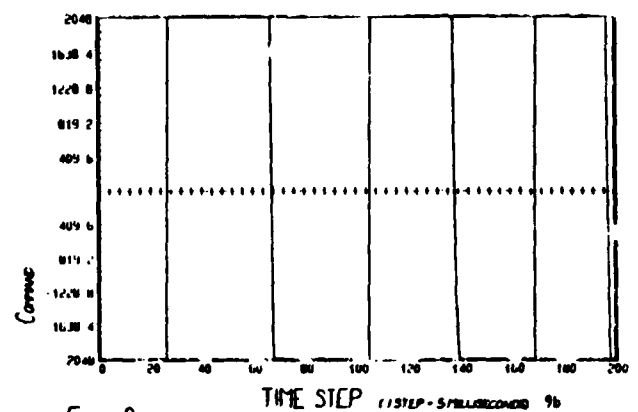
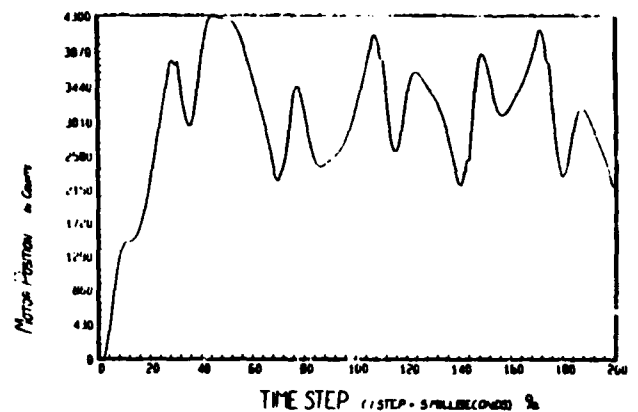


FIGURE 9 Experimental Motor Position and Command for Derivative Control

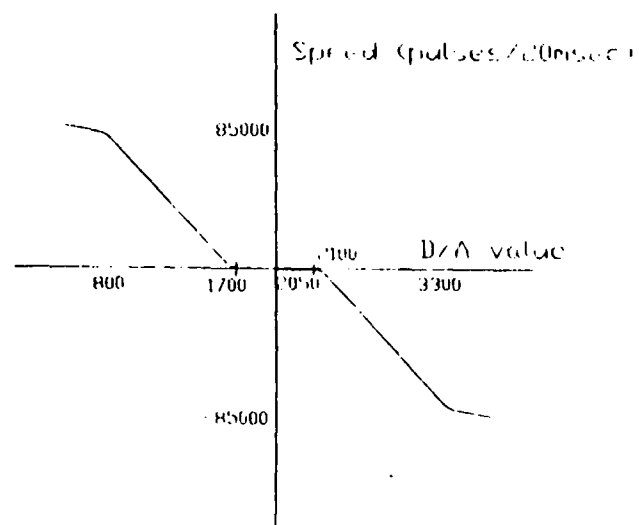


Fig. 10 Steady State Velocity vs. Discrete Torque Command Level

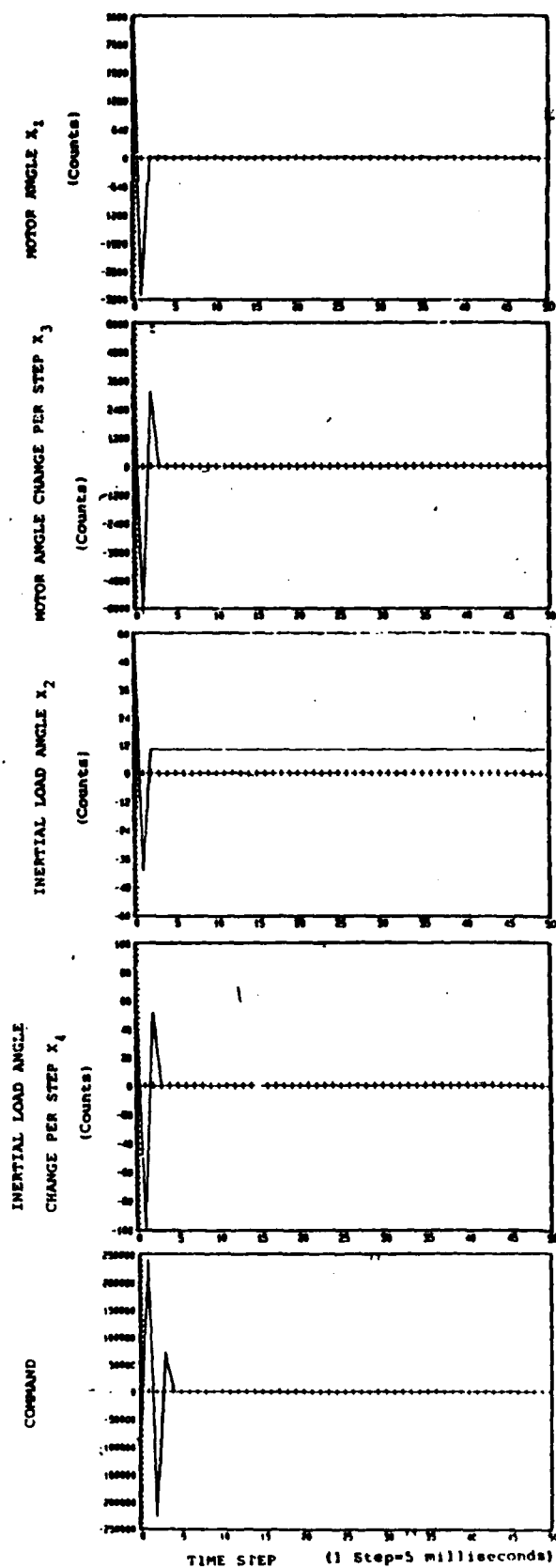


Fig. 11. Deadbeat Control Simulation of Identified System Model.

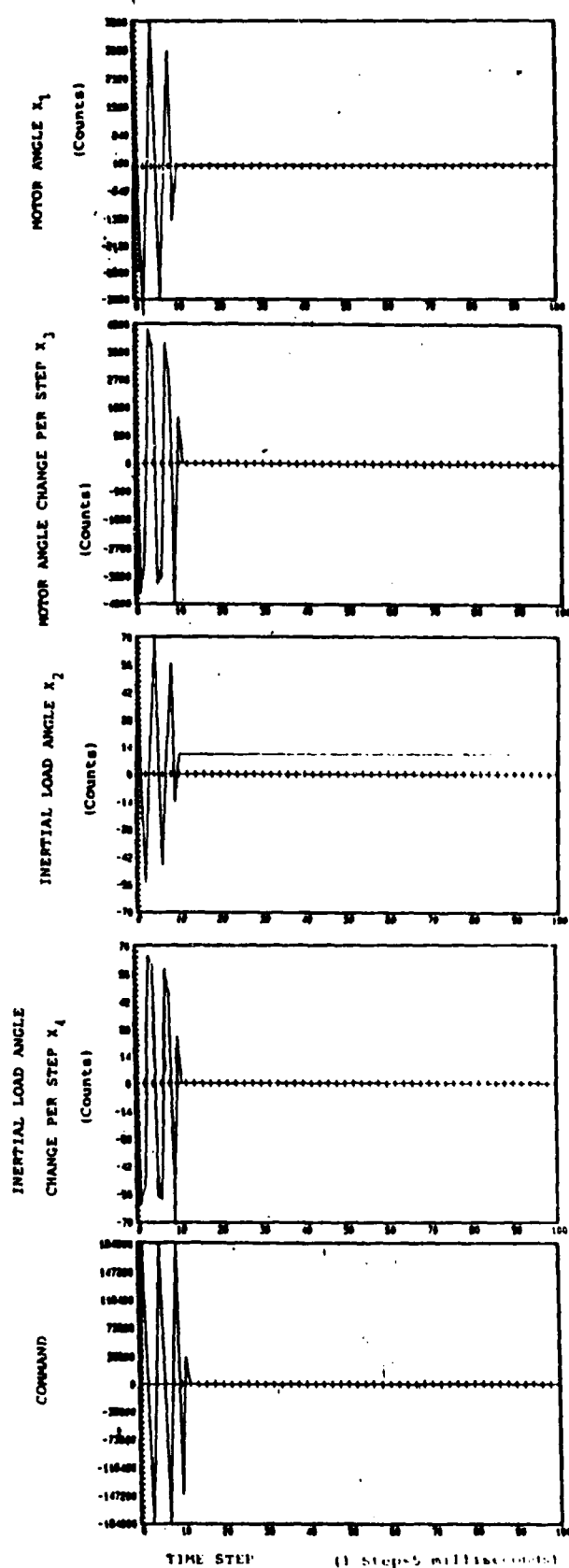


Fig. 12. Deadbeat Control Simulation with Control Saturation at 184,000 Counts.

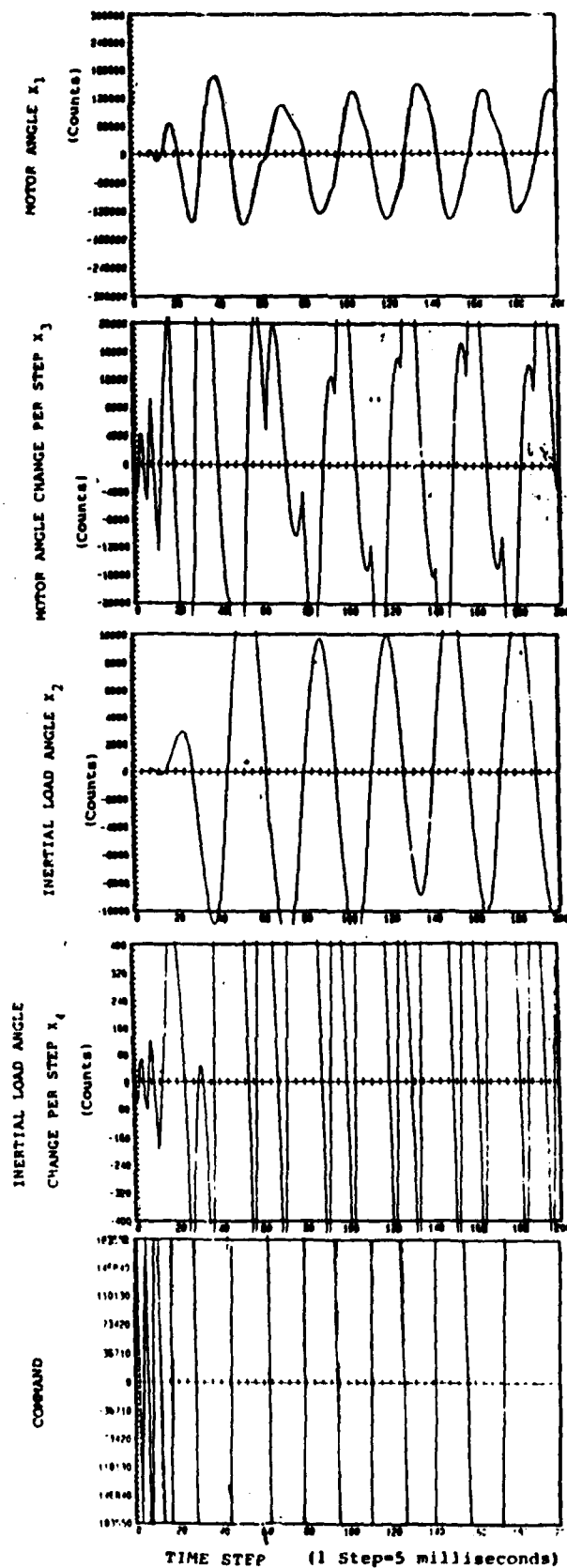


Fig. 13. Deadbeat Control Simulation with Control Saturation at 183,500 Counts.

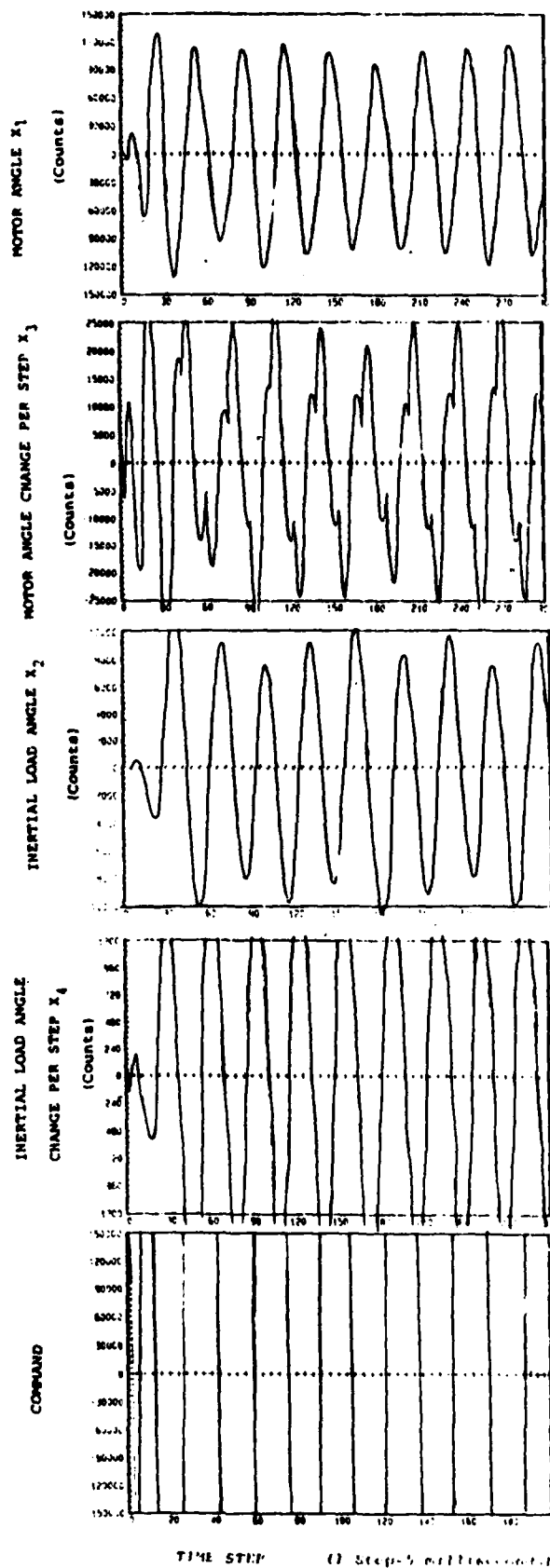


Fig. 14. Deadbeat Control Simulation with Control Saturation at 150,000 Counts.

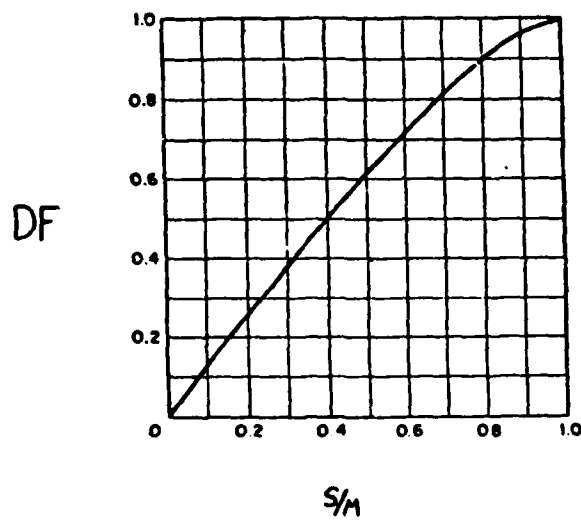


FIGURE 15 THE DESCRIBING FUNCTION FOR A SATURATION NONLINEARITY.

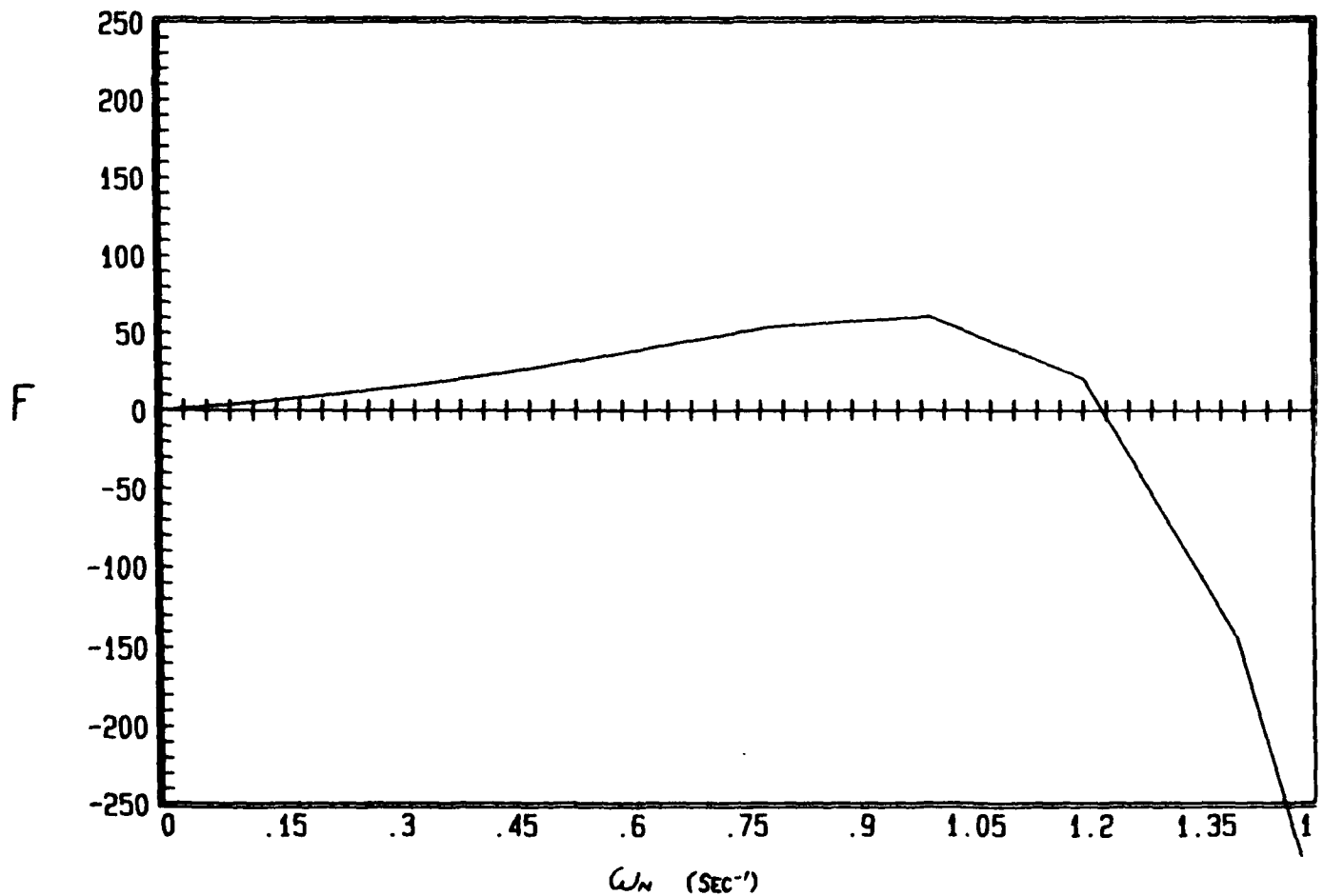


FIGURE 16 DETERMINATION OF LIMIT CYCLE FREQUENCY ω_N BY PLOTTING $F(\omega_N)$ FROM EQUATION ().